

UC Irvine

UC Irvine Previously Published Works

Title

Supergravity with a gravitino lightest supersymmetric particle

Permalink

<https://escholarship.org/uc/item/5pd6z2xj>

Journal

Physical Review D, 70(7)

ISSN

2470-0010

Authors

Feng, Jonathan L
Su, Shufang
Takayama, Fumihiro

Publication Date

2004-10-01

DOI

10.1103/physrevd.70.075019

Copyright Information

This work is made available under the terms of a Creative Commons Attribution License, available at <https://creativecommons.org/licenses/by/4.0/>

Peer reviewed

Supergravity with a gravitino lightest supersymmetric particle

Jonathan L. Feng,¹ Shufang Su,² and Fumihiro Takayama¹¹*Department of Physics and Astronomy, University of California, Irvine, California 92697, USA*²*Department of Physics, University of Arizona, Tucson, Arizona 85721, USA*

(Received 26 May 2004; published 25 October 2004)

We investigate supergravity models in which the lightest supersymmetric particle (LSP) is a stable gravitino. We assume that the next-lightest supersymmetric particle (NLSP) freezes out with its thermal relic density before decaying to the gravitino at time $t \sim 10^4 - 10^8$ s. In contrast to studies that assume a fixed gravitino relic density, the thermal relic density assumption implies upper, not lower, bounds on superpartner masses, with important implications for particle colliders. We consider slepton, sneutrino, and neutralino NLSPs, and determine what superpartner masses are viable in all of these cases, applying cosmic microwave background (CMB) and electromagnetic and hadronic big bang nucleosynthesis (BBN) constraints to the leading two- and three-body NLSP decays. Hadronic constraints have been neglected previously, but we find that they provide the most stringent constraints in much of the natural parameter space. We then discuss the collider phenomenology of supergravity with a gravitino LSP. We find that colliders may provide important insights to clarify BBN and the thermal history of the Universe below temperatures around 10 GeV and may even provide precise measurements of the gravitino's mass and couplings.

DOI: 10.1103/PhysRevD.70.075019

PACS numbers: 04.65.+e, 12.60.Jv, 26.35.+c, 98.80.Es

I. INTRODUCTION

Supersymmetric theories predict the existence of a spin 3/2 particle, the gravitino, the partner of the spin two graviton. The gravitino mass is

$$m_{\tilde{G}} \sim \frac{F}{M_*}, \quad (1)$$

where F is the scale of supersymmetry breaking, and $M_* = (8\pi G_N)^{-1/2} \simeq 2.4 \times 10^{18}$ GeV is the reduced Planck mass. The masses of scalar superpartners are derived from terms such as

$$\lambda_{ij} \int d^4\theta \frac{Z^\dagger Z \Phi_i^\dagger \Phi_j}{M_{\text{med}}^2}, \quad (2)$$

where λ_{ij} are unknown constants, Z is a superfield whose auxiliary component develops the vacuum expectation value F , Φ_i are standard model superfields, and M_{med} is the mass scale of the interactions that mediate supersymmetry breaking. Similar terms give the spin 1/2 superpartners mass. In supergravity, the mediating interactions are gravitational, and so $M_{\text{med}} \sim M_*$, $F \sim (10^{10} \text{ GeV})^2$, and the gravitino and all standard model superpartners have mass $\sim F/M_* \sim M_{\text{weak}}$, with the precise ordering determined by unknown constants, such as λ_{ij} .

Most studies of supergravity have assumed, either explicitly or implicitly, that the lightest supersymmetric particle (LSP) is a standard model superpartner. This avoids potential complications resulting from the decay of standard model superpartners to a gravitino LSP, which naturally happens at time $t \sim 10^4 - 10^8$ s, well after big bang nucleosynthesis (BBN). However, the phenomenology and cosmology of gravitinos have also been consid-

ered in a number of studies [1–12]. (See also related studies of axino and quintessino dark matter [13–16].)

More recently, it has been shown that the gravitino LSP possibility does not destroy the beautiful predictions of BBN even when the gravitino LSPs produced in late decays have relic density $\Omega_{\tilde{G}} = 0.23$ and so are present in sufficient numbers to account for all of dark matter [17–19]. In fact, bounds from the cosmic microwave background (CMB) and, in some corners of parameter space, entropy production and the diffuse photon spectrum may be even more severe than bounds from BBN [17,18]. Nevertheless, all of these bounds were shown to be respected for some regions of parameter space with weak-scale superpartners. The possibility of superweakly-interacting massive particle (superWIMP) gravitino dark matter from NLSP decays thus appears to be viable. The analogous scenario in extra dimensional theories [17,18,20], as well as interesting astrophysical implications in this and related scenarios [15,21,22] have also been discussed.

In this work, we take an approach that differs from the exploration of superWIMP gravitino dark matter. Instead of assuming that gravitinos are the dark matter with $\Omega_{\tilde{G}} = 0.23$, we assume that the NLSP reaches its thermal relic density $\Omega_{\text{NLSP}}^{\text{th}}$ before decaying, and so $\Omega_{\tilde{G}} = (m_{\tilde{G}}/m_{\text{NLSP}})\Omega_{\text{NLSP}}^{\text{th}}$. That is, we relax the constraint that gravitinos from NLSP decays account for all of dark matter. Rather we assume the simplest thermal history for the Universe and ask what regions of $(m_{\tilde{G}}, m_{\text{NLSP}})$ parameter space are allowed. The thermal relic density assumption has consequences that differ markedly from the fixed gravitino relic density assumption. To see this, assume that the gravitino and NLSP masses are both parametrized by a general superpartner mass scale

m_{SUSY} . As noted in Ref. [19], if one assumes a fixed gravitino relic density, the NLSP number density scales as $1/m_{\text{SUSY}}$. Low superpartner masses are therefore disfavored. In contrast, if one assumes a thermal relic density for the NLSP, $\Omega_{\text{NLSP}}^{\text{th}} \propto \langle \sigma v \rangle^{-1} \propto m_{\text{SUSY}}^2$, where $\langle \sigma v \rangle$ is the thermally-averaged NLSP annihilation cross section. The NLSP number density then scales as m_{SUSY} , and so high superpartner masses are disfavored. This difference has obviously important implications for collider searches for new physics, and we discuss collider implications below.

Even given the NLSP thermal relic density assumption, gravitinos may still be all of dark matter—for example, if the gravitino relic density from NLSP decays is too low, the remainder may be made up by gravitinos produced during reheating. However, the existence of such alternative gravitino sources is either untestable, or testable only with strong assumptions about the early Universe. In contrast, the existence of a gravitino component from NLSP decays makes several robust predictions that are testable at cosmological observatories and collider experiments, and we concentrate on this gravitino source here. Before leaving the topic of reheating altogether, however, we note that the gravitino LSP scenario has an important virtue with respect to reheating. For stable weak-scale gravitinos, the overclosure constraint is well known to require a bound on reheat temperature of $T_R \lesssim 10^{10}$ GeV [11]. Recently, however, it has been shown that if the gravitino is not the LSP, hadronic BBN constraints greatly strengthen this bound [23]. For example, if the gravitino decays to the LSP + hadrons with branching fraction 10^{-3} , the reheat temperature must satisfy $T_R \lesssim 10^6$ GeV. This is uncomfortably low. The gravitino LSP scenario is therefore preferred if one requires a high reheat temperature, as might be desirable, for example, for scenarios of leptogenesis [24].

In the present analysis, in addition to the constraints on electromagnetic energy release considered previously, we include the recent results on hadronic BBN constraints [23]. The work of Ref. [23] represents a significant update to previous hadronic analyses [25–28]. To include these results correctly, we must, of course, determine the leading contributions to hadronic energy. For slepton¹ and sneutrino NLSPs, the leading contribution is from three-body decays

$$\tilde{l} \rightarrow lZ\tilde{G}, \quad \nu W\tilde{G}; \quad \tilde{\nu} \rightarrow \nu Z\tilde{G}, \quad lW\tilde{G}. \quad (3)$$

The three-body decays have been studied in Ref. [19]. For a neutralino NLSP, the leading contribution to hadronic energy is from the two-body decays, such as

$$\chi \rightarrow Z\tilde{G}, \quad h\tilde{G}, \quad (4)$$

followed by $Z, h \rightarrow q\bar{q}$. These decays, and the hadronic

constraints on them, were neglected in previous works. As we will see, however, they are the leading constraints in much of parameter space and they are especially important when the superpartner masses and their splittings are all of the order of the weak-scale, the most natural possibility.

The decays of Eqs. (3) and (4) may be suppressed kinematically if $m_{\text{NLSP}} - m_{\tilde{G}} < m_Z, m_W$ or dynamically, as when the neutralino is photinolike. However, even in these cases, decays such as $\tilde{l} \rightarrow lq\bar{q}\tilde{G}$ and $\chi \rightarrow q\bar{q}\tilde{G}$ are still possible at higher order. We have included estimates of these in our analysis. These decays are in some sense “model independent”; even in the extreme case where the dominant decay is to invisible particles, at higher order there will be contributions to hadronic cascades from such decays. The hadronic bounds are so constraining that these should be considered for any late decaying particle, whether a superpartner, an axino, a modulus, or an other particle.

After determining the regions of parameter space allowed by cosmology, we discuss the collider signals. The upper bounds on superpartner masses resulting from the thermal relic density assumption imply promising prospects for superpartners to be within reach of future collider experiments. In addition, we will see that the signals of supersymmetry in gravitino LSP scenarios may be completely different from the conventional supersymmetry signals. In particular, if sufficient NLSPs can be collected and monitored for decays, the NLSP lifetime may be measured, which may considerably sharpen our understanding of BBN and the thermal history of the Universe at temperatures of 10 GeV and below. Such studies may also provide the first direct measurements of the gravitino mass and the Planck scale from particle physics [29,30].

The gravitino LSP possibility, assuming a thermal NLSP relic density, has been discussed recently in the context of minimal supergravity [31]. Our work is complementary in that we do not work in a specific model framework, but rather consider several NLSP candidates, as well as a wide range of gravitino and NLSP masses. Our work also differs in that we consider the hadronic constraints and the leading two- and three-body decays that contribute to hadronic energy. As noted above, we find that these are the leading constraints in the most natural regions of parameter space.

II. LATE DECAYS

We first discuss the decays of NLSPs for each of the various NLSP cases. NLSPs freeze out and are highly nonrelativistic when they decay. We will be most interested in deriving the electromagnetic (EM) and hadronic energy releases

$$\xi_i \equiv \epsilon_i B_i Y_{\text{NLSP}}, \quad (5)$$

¹Throughout this work, “slepton” refers to a charged slepton.

where $i = \text{EM, had}$, because BBN constraints are, to a good approximation, constraints on ξ_{EM} and ξ_{had} . Here B_i is the branching fraction into EM/hadronic components, and ϵ_i is the EM/hadronic energy released in each NLSP decay. These are discussed in this section. $Y_{\text{NLSP}} \equiv n_{\text{NLSP}}/n_{\gamma}^{\text{BG}}$ is the NLSP number density just before NLSP decay, normalized to the background photon number density $n_{\gamma}^{\text{BG}} = 2\zeta(3)T^3/\pi^2$.² Given the assumptions of this work, Y_{NLSP} is determined by the thermal relic density for each NLSP; it is discussed in Sec. III.

We will consider the cases of slepton, sneutrino, and neutralino NLSPs. As specific examples in each of these categories, we will focus on $\tilde{\tau}_R$, $\tilde{\nu}_\tau$, and \tilde{B} NLSPs, but our results are easily extended to the general cases.

A. Slepton NLSP

The width for the decay of any sfermion to a gravitino is

$$\Gamma(\tilde{f} \rightarrow f\tilde{G}) = \frac{1}{48\pi M_*^2} \frac{m_{\tilde{f}}^5}{m_{\tilde{G}}^2} \left[1 - \frac{m_{\tilde{G}}^2}{m_{\tilde{f}}^2} \right]^4, \quad (6)$$

assuming the fermion mass is negligible. For $\Delta m \equiv m_{\tilde{f}} - m_{\tilde{G}} \ll m_{\tilde{G}}$, the sfermion decay lifetime is

$$\tau(\tilde{f} \rightarrow f\tilde{G}) \approx 3.6 \times 10^8 \text{s} \left[\frac{100 \text{ GeV}}{\Delta m} \right]^4 \left[\frac{m_{\tilde{G}}}{1 \text{ TeV}} \right]. \quad (7)$$

The slepton lifetime and mass are given in the $(m_{\tilde{G}}, \delta m)$ plane in Fig. 1, where we have defined

$$\delta m \equiv \Delta m - m_Z = m_{\text{NLSP}} - m_{\tilde{G}} - m_Z, \quad (8)$$

a useful measure of the kinematically available energy in three-body decays to be discussed below.

For selectrons, the produced electron in these two-body decays immediately initiates an electromagnetic (EM) cascade, and so

$$B_{\text{EM}}^{\tilde{e}} \approx 1, \quad \epsilon_{\text{EM}}^{\tilde{e}} = \frac{m_{\tilde{e}}^2 - m_{\tilde{G}}^2}{2m_{\tilde{e}}}. \quad (9)$$

For smuons, the produced muon typically interacts with the background photons before decaying [18], and so

$$B_{\text{EM}}^{\tilde{\mu}} \approx 1, \quad \epsilon_{\text{EM}}^{\tilde{\mu}} = \frac{m_{\tilde{\mu}}^2 - m_{\tilde{G}}^2}{2m_{\tilde{\mu}}}. \quad (10)$$

For staus, the resulting τ sometimes decays into mesons, which could in principle induce hadronic cascades. As shown in Refs. [18,19], however, for decay times $\tau > 10^3 - 10^4$ s, the hadronic interaction time of all pions and kaons is much longer than their decay time. The decays of staus therefore typically contribute only to EM cascades, and we assume this in the following analysis. In contrast to the selectron and smuon cases, however,

²Another common definition is $Y_{\text{NLSP}} \equiv n_{\text{NLSP}}/s$, where $s = (2\pi^2/45)g_*T^3$ is the entropy density. In the era of NLSP decays to gravitinos, $s \approx 7.0n_{\gamma}^{\text{BG}}$.

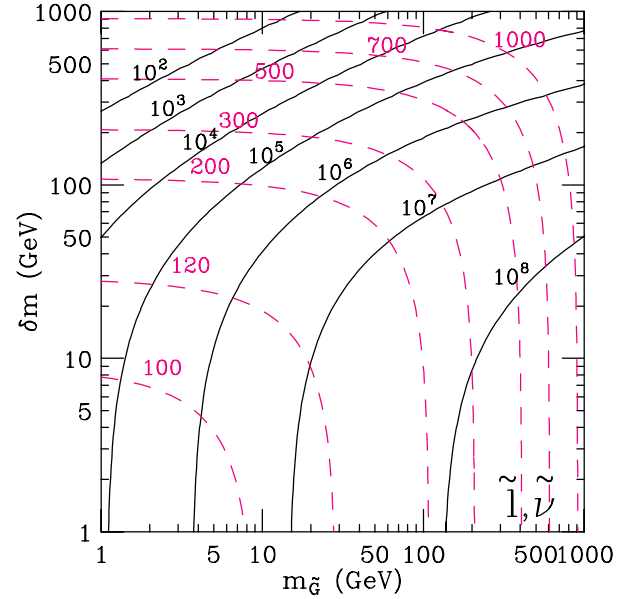


FIG. 1 (color online). NLSP lifetime in seconds (solid lines) and mass in GeV (dashed lines) in the $(m_{\tilde{G}}, \delta m \equiv m_{\text{NLSP}} - m_{\tilde{G}} - m_Z)$ plane for slepton and sneutrino NLSPs.

on average, about half of the τ energy is lost to neutrinos. We therefore have

$$B_{\text{EM}}^{\tilde{\tau}} \approx 1, \quad \epsilon_{\text{EM}}^{\tilde{\tau}} \approx \frac{1}{2} \frac{m_{\tilde{\tau}}^2 - m_{\tilde{G}}^2}{2m_{\tilde{\tau}}}. \quad (11)$$

As noted in Sec. I, three-body decays are also important when they are the leading contribution to hadronic cascades. They are therefore important for slepton NLSPs. The decays are those of Eq. (3). The decay $\tilde{l} \rightarrow lZ\tilde{G}$ takes place through off shell l , \tilde{l} , and χ , and also through a four-point interaction. The three-body decay widths for sleptons have been discussed and presented in Ref. [19], and we refer readers there for details. Given these decay widths, the hadronic branching fraction is

$$B_{\text{had}}^{\tilde{l}} \approx \frac{\Gamma(\tilde{l} \rightarrow lZ\tilde{G})B_{\text{had}}^Z + \Gamma(\tilde{l} \rightarrow \nu W\tilde{G})B_{\text{had}}^W + \Gamma(\tilde{l} \rightarrow lq\tilde{G})}{\Gamma(\tilde{l} \rightarrow l\tilde{G})}, \quad (12)$$

for $\tilde{l} = \tilde{e}, \tilde{\mu}, \tilde{\tau}$, where $B_{\text{had}}^Z, B_{\text{had}}^W \approx 0.7$ are the Z and W hadronic branching fractions. $\Gamma(\tilde{l} \rightarrow \nu W\tilde{G}) = 0$ for purely right-handed sleptons. Below, we will consider cases in which the three-body decays are kinematically allowed. These decay modes may nevertheless become suppressed for $\Delta m \sim m_Z, m_W$. However, even for such small mass splittings, hadronic decays are still possible through higher order decays. With this in mind, we have included the four-body process $\Gamma(\tilde{l} \rightarrow lq\tilde{G})$. We have not calculated this width. However, we expect $B(\tilde{l} \rightarrow lq\tilde{G}) \sim 10^{-6}$, and we take this value, which provides a lower limit on $B_{\text{had}}^{\tilde{l}}$.

$B_{\text{had}}^{\tilde{l}}$ is typically in the range $10^{-2} - 10^{-5}$, depending on the underlying scale and mass splitting. As the branching fraction may vary over a few orders of magnitude, variations in $\epsilon_{\text{had}}^{\tilde{l}}$ are subdominant. We therefore take simply

$$\epsilon_{\text{had}}^{\tilde{l}} = \frac{1}{3}(m_{\tilde{l}} - m_{\tilde{G}}) \quad (13)$$

in our analysis.

B. Sneutrino NLSP

The decay width and time for $\tilde{\nu} \rightarrow \nu \tilde{G}$ are given in Eqs. (6) and (7), and plotted in Fig. 1. These two-body decays are essentially invisible and do not contribute to either EM or hadronic cascades. (We neglect the effects of neutrino thermalization through processes like $\nu e_{\text{BG}} \rightarrow \nu e$.) The three-body decays are therefore even more important for sneutrinos than sleptons. These decays have also been discussed and presented in Ref. [19]. For sneutrinos, we have

$$B_{\text{EM}}^{\tilde{\nu}} \simeq \frac{\Gamma(\tilde{\nu} \rightarrow \nu Z \tilde{G}) + \Gamma(\tilde{\nu} \rightarrow l W \tilde{G}) + \Gamma(\tilde{\nu} \rightarrow \nu f \tilde{f} \tilde{G})}{\Gamma(\tilde{\nu} \rightarrow \nu \tilde{G})}, \quad (14)$$

$$\epsilon_{\text{EM}}^{\tilde{\nu}} = \frac{1}{3}(m_{\tilde{\nu}} - m_{\tilde{G}}), \quad (15)$$

$$B_{\text{had}}^{\tilde{\nu}} \simeq \frac{\Gamma(\tilde{\nu} \rightarrow \nu Z \tilde{G}) B_{\text{had}}^Z + \Gamma(\tilde{\nu} \rightarrow l W \tilde{G}) B_{\text{had}}^W + \Gamma(\tilde{\nu} \rightarrow \nu q \tilde{q} \tilde{G})}{\Gamma(\tilde{\nu} \rightarrow \nu \tilde{G})}, \quad (16)$$

$$\epsilon_{\text{had}}^{\tilde{\nu}} = \frac{1}{3}(m_{\tilde{\nu}} - m_{\tilde{G}}), \quad (17)$$

for $\tilde{\nu} = \tilde{\nu}_e, \tilde{\nu}_\mu, \tilde{\nu}_\tau$. The EM branching fraction is in fact slightly reduced by decays $\tilde{\nu} \rightarrow \nu Z \tilde{G}$ followed by $Z \rightarrow \nu \bar{\nu}$. We have neglected this effect. The four-body decay takes place through virtual neutralinos. We again assume $B(\tilde{\nu} \rightarrow \nu q \tilde{q} \tilde{G}) \sim 10^{-6}$, which provides a lower limit on $B_{\text{had}}^{\tilde{\nu}}$.

Note that, in contrast to the case of the slepton NLSP, the EM branching fraction is suppressed and of the same order as the hadronic branching fraction. In our analysis below we have included the EM constraint, but we find that it is so weak that it does not disfavor any of the parameter space appearing in figures below. The hadronic BBN constraint is so much stronger than the EM constraint at early times, however, that it is still important then, as we will see.

C. Neutralino NLSP

For neutralino NLSPs, the decay width to photons is

$$\Gamma(\chi \rightarrow \gamma \tilde{G}) = \frac{|N_{11} \cos\theta_W + N_{12} \sin\theta_W|^2 m_\chi^5}{48\pi M_*^2 m_{\tilde{G}}^2} \times \left[1 - \frac{m_{\tilde{G}}^2}{m_\chi^2} \right]^3 \left[1 + 3 \frac{m_{\tilde{G}}^2}{m_\chi^2} \right], \quad (18)$$

where $\chi \equiv \mathbf{N}_{11}(-i\tilde{B}) + \mathbf{N}_{12}(-i\tilde{W}) + \mathbf{N}_{13}\tilde{H}_d + \mathbf{N}_{14}\tilde{H}_u$. In the limit $\Delta m \ll m_\chi$, the decay lifetime is

$$\tau(\chi \rightarrow \gamma \tilde{G}) \approx 2.3 \times 10^7 \text{s} \frac{\cos^2\theta_W}{|N_{11} \cos\theta_W + N_{12} \sin\theta_W|^2} \times \left[\frac{100 \text{ GeV}}{\Delta m} \right]^3, \quad (19)$$

proportional to $(\Delta m)^3$ and independent of the overall superpartner mass scale.

This decay contributes only to EM energy. As noted in Sec. I, the leading contribution to hadronic energy is from $\chi \rightarrow Z \tilde{G}, h \tilde{G}$. These decays produce EM energy for all possible Z and h decay modes (except $Z \rightarrow \nu \bar{\nu}$), but they may also produce hadronic energy when followed by $Z, h \rightarrow q \bar{q}$. The decay width to Z bosons is³

$$\Gamma(\chi \rightarrow Z \tilde{G}) = \frac{|-N_{11} \sin\theta_W + N_{12} \cos\theta_W|^2 m_\chi^5}{48\pi M_*^2 m_{\tilde{G}}^2} \times F(m_\chi, m_{\tilde{G}}, m_Z) \times \left[\left(1 - \frac{m_{\tilde{G}}^2}{m_\chi^2} \right)^2 \left(1 + 3 \frac{m_{\tilde{G}}^2}{m_\chi^2} \right) - \frac{m_Z^2}{m_\chi^2} G(m_\chi, m_{\tilde{G}}, m_Z) \right], \quad (20)$$

where

$$F(m_\chi, m_{\tilde{G}}, m_Z) = \left(\left[1 - \left(\frac{m_{\tilde{G}} + m_Z}{m_\chi} \right)^2 \right] \times \left[1 - \left(\frac{m_{\tilde{G}} - m_Z}{m_\chi} \right)^2 \right] \right)^{1/2}, \quad (21)$$

$$G(m_\chi, m_{\tilde{G}}, m_Z) = 3 + \frac{m_{\tilde{G}}^3}{m_\chi^3} \left(-12 + \frac{m_{\tilde{G}}}{m_\chi} \right) + \frac{m_Z^4}{m_\chi^4} - \frac{m_Z^2}{m_\chi^2} \left(3 - \frac{m_{\tilde{G}}^2}{m_\chi^2} \right). \quad (22)$$

³Our expression for G in Eq. (22) differs from the result of Ref. [31] in the sign of “12” in the second term. The authors of Ref. [31] used Eq. (4.31) of Ref. [32], which contains a sign error. We have corrected for this error. We thank Y. Santoso and T. Moroi for helpful correspondence.

The decay width to the Higgs boson is⁴

$$\begin{aligned} \Gamma(\chi \rightarrow h\tilde{G}) &= \frac{|-N_{13}\sin\alpha + N_{14}\cos\alpha|^2}{96\pi M_*^2} \frac{m_\chi^5}{m_{\tilde{G}}^2} \\ &\times F(m_\chi, m_{\tilde{G}}, m_h) \left[\left(1 - \frac{m_{\tilde{G}}}{m_\chi}\right)^2 \right. \\ &\times \left. \left(1 + \frac{m_{\tilde{G}}}{m_\chi}\right)^4 - \frac{m_h^2}{m_\chi^2} H(m_\chi, m_{\tilde{G}}, m_h) \right], \end{aligned} \quad (23)$$

where $h = (-H_d^0 \sin\alpha + H_u^0 \cos\alpha)/\sqrt{2}$, F is as given in Eq. (21), and

$$\begin{aligned} H(m_\chi, m_{\tilde{G}}, m_h) &= 3 + 4\frac{m_{\tilde{G}}}{m_\chi} + 2\frac{m_{\tilde{G}}^2}{m_\chi^2} + 4\frac{m_{\tilde{G}}^3}{m_\chi^3} + 3\frac{m_{\tilde{G}}^4}{m_\chi^4} + \frac{m_h^4}{m_\chi^4} \\ &- \frac{m_h^2}{m_\chi^2} \left(3 + 2\frac{m_{\tilde{G}}}{m_\chi} + 3\frac{m_{\tilde{G}}^2}{m_\chi^2}\right). \end{aligned} \quad (24)$$

For the case of a Bino-like neutralino, the neutralino's mass and lifetime are given in the $(m_{\tilde{G}}, \delta m)$ plane in Fig. 2.

Given these two-body decay widths, the resulting values for the energy release parameters are

$$B_{\text{EM}}^\chi \approx 1, \quad (25)$$

$$\epsilon_{\text{EM}}^\chi = \frac{m_\chi^2 - m_{\tilde{G}}^2}{2m_\chi}, \quad (26)$$

$$B_{\text{had}}^\chi \approx \frac{\Gamma(\chi \rightarrow Z\tilde{G})B_{\text{had}}^Z + \Gamma(\chi \rightarrow h\tilde{G})B_{\text{had}}^h + \Gamma(\chi \rightarrow q\bar{q}\tilde{G})}{\Gamma(\chi \rightarrow \gamma\tilde{G}) + \Gamma(\chi \rightarrow Z\tilde{G}) + \Gamma(\chi \rightarrow h\tilde{G})}, \quad (27)$$

$$\epsilon_{\text{had}}^\chi \approx \frac{m_\chi^2 - m_{\tilde{G}}^2 + m_{Z,h}^2}{2m_\chi}, \quad (28)$$

where $B_{\text{had}}^h \approx 0.9$. For the three-body decay, we take $\Gamma(\chi \rightarrow q\bar{q}\tilde{G}) \sim 10^{-3}$, which provides a lower bound on B_{had}^χ when the two-body decays become kinematically suppressed. In addition, for $m_\chi - m_{\tilde{G}} < m_Z$, $\epsilon_{\text{had}}^\chi$ is estimated to be $\frac{2}{3}(m_\chi - m_{\tilde{G}})$ in our analyses.

We have neglected decays to the heavy Higgs bosons. When kinematically allowed, they will, of course, modify the branching fraction and energy release formulae above. The decay width to the heavy CP -even Higgs boson H is given by replacing $m_h \rightarrow m_H$ and $-N_{13}\sin\alpha + N_{14}\cos\alpha \rightarrow N_{13}\cos\alpha + N_{14}\sin\alpha$ in Eq. (23). The decay width to the CP -odd Higgs boson A is given by replacing $m_h \rightarrow m_A$, $-N_{13}\sin\alpha + N_{14}\cos\alpha \rightarrow N_{13}\sin\beta + N_{14}\cos\beta$ and, in the last two lines of Eq. (23),

⁴This result disagrees with the decay width given in Ref. [31]. After cross-checking with the authors, they agree with our current results. We thank Y. Santoso and V. Spanos for helpful correspondence.

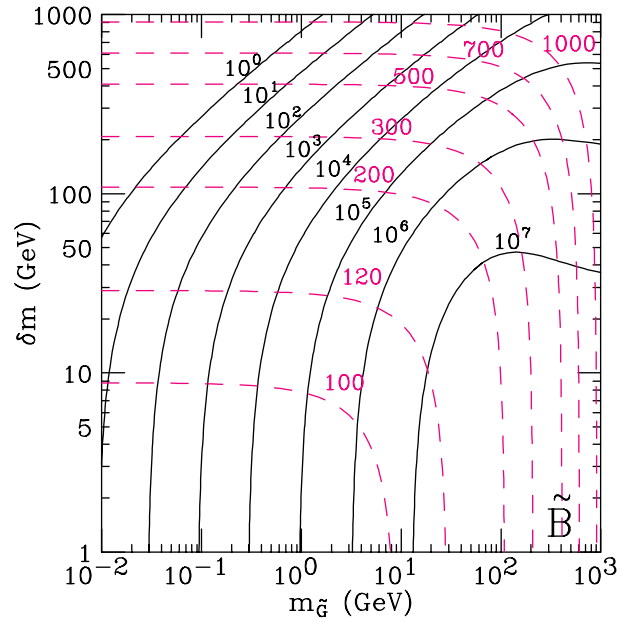


FIG. 2 (color online). As in Fig. 1, but for a Bino NLSP.

$m_\chi \rightarrow -m_\chi$, where the last transformation is required by the CP -odd nature of the A boson.

III. THERMAL RELIC DENSITIES

To determine the normalized NLSP number density Y_{NLSP} of Eq. (5) and also the resulting contribution of gravitinos to the current dark matter energy density, we assume that the NLSP freezes out with its thermal relic density. The superWIMP has no effect on the early thermal history of the Universe. The NLSP therefore freezes out as usual, with relic density given approximately by [33,34]

$$\begin{aligned} \Omega_{\text{NLSP}}^{\text{th}} h^2 &\approx \frac{1.1 \times 10^9 x_F \text{ GeV}^{-1}}{\sqrt{g_*} M_{\text{Pl}} c_J \langle \sigma v \rangle} \\ &\approx 0.2 \left[\frac{15}{\sqrt{g_*}} \right] \left[\frac{x_F}{30} \right] \left[\frac{10^{19} \text{ GeV}}{M_{\text{Pl}}} \right] \left[\frac{10^{-9} \text{ GeV}^{-2}}{c_J \langle \sigma v \rangle} \right], \end{aligned} \quad (29)$$

where $x_F = m_{\text{NLSP}}/T_F$ is the NLSP mass divided by the freeze out temperature T_F , g_* is the effective number of massless degrees of freedom at freeze out, and $\langle \sigma v \rangle$ is the thermally-averaged NLSP annihilation cross section, and c_J is 1 for S -wave annihilation, 1/2 for P -wave annihilation. The energy release parameter Y_{NLSP} is derived from this through

$$Y_{\text{NLSP}} = \frac{\Omega_{\text{NLSP}}^{\text{th}} \rho_c}{m_{\text{NLSP}} n_\gamma^{\text{BG}}} \approx 1.3 \times 10^{-11} \left[\frac{\text{TeV}}{m_{\text{NLSP}}} \right] \Omega_{\text{NLSP}}^{\text{th}}, \quad (30)$$

and the gravitino relic density is given by

$$\Omega_{\tilde{G}} h^2 = \frac{m_{\tilde{G}}}{m_{\text{NLSP}}} \Omega_{\text{NLSP}}^{\text{th}} h^2. \quad (31)$$

For the case of slepton NLSPs, the dominant annihilation channels are typically $\tilde{l}\tilde{l}^* \rightarrow \gamma\gamma, \gamma Z, ZZ$ through slepton exchange and $\tilde{l}\tilde{l} \rightarrow ll$ through Bino exchange. For right-handed sleptons, the thermally-averaged cross section near threshold may be approximated as [35]

$$\begin{aligned} \langle\sigma v\rangle_{\tilde{l}_R} &\approx \frac{4\pi\alpha^2}{m_{\tilde{l}_R}^2} + \frac{16\pi\alpha^2 m_{\tilde{B}}^2}{\cos^4\theta_W(m_{\tilde{l}_R}^2 + m_{\tilde{B}}^2)^2} \\ &= 5.0 \times 10^{-10} C \left[\frac{\text{TeV}}{m_{\tilde{l}_R}} \right]^2 \text{GeV}^{-2}, \end{aligned} \quad (32)$$

where $m_{\tilde{B}}, m_{\tilde{l}_R}$ are the Bino and slepton masses, respectively, and C is an $\mathcal{O}(1)$ model-dependent constant. Here we have not included coannihilation processes, which might be important if sleptons and, say, neutralinos are nearly mass degenerate. Using Eq. (29) and setting $C = 1$, the slepton thermal relic abundance is

$$\Omega_{\tilde{l}_R}^{\text{th}} h^2 \approx 0.2 \left[\frac{m_{\tilde{l}_R}}{\text{TeV}} \right]^2. \quad (33)$$

A similar analysis for the sneutrino NLSP case yields [24]

$$\Omega_{\tilde{\nu}}^{\text{th}} h^2 \approx 0.06 \left[\frac{m_{\tilde{\nu}}}{\text{TeV}} \right]^2. \quad (34)$$

The thermal relic density of the sneutrino is typically smaller than that of right-handed sleptons because sneutrino annihilation is relatively efficient, taking place through weak SU(2) couplings, whereas the right-handed sleptons annihilate only through hypercharge couplings.

For the neutralino NLSP case, the thermal relic density is very model-dependent. The annihilation cross section varies widely depending on the gaugino-Higgsino composition of the neutralino and the presence or absence of coannihilation effects, and so depends on a large number of unknown supersymmetry parameters. Rather than constraining these parameters by working in a particular model, we adopt a simple scaling behavior based on some well-known results. In particular, we assume that the annihilation cross section scales as $m_{\tilde{\chi}}^{-2}$. To fix the constant of proportionality, we recall that in the ‘‘bulk’’ region of minimal supergravity, where the neutralino is Bino-like and there is no significant coannihilation, the desired relic density is achieved for $m_{\tilde{B}} \approx 100$ GeV. In the focus point (FP) region of minimal supergravity [36–38], where the neutralino is a Bino-Higgsino mixture [39], the neutralino mass may be much larger [40,41]. If there are coannihilation effects [42,43], the neutralino mass may also be much higher [44–46]. To study the effect of having a heavier neutralino, we consider the mass $m_{\tilde{B}} \approx 200$ GeV as an example of these other possibilities. We therefore consider the range

$$\text{bulk : } \Omega_{\tilde{\chi}}^{\text{th}} h^2 \approx 0.1 \left[\frac{m_{\tilde{\chi}}}{100 \text{ GeV}} \right]^2, \quad (35)$$

to

focus point/coannihilation :

$$\Omega_{\tilde{\chi}}^{\text{th}} h^2 \approx 0.1 \left[\frac{m_{\tilde{\chi}}}{200 \text{ GeV}} \right]^2. \quad (36)$$

Note that for similar NLSP masses, the thermal relic density is much higher in the neutralino case than in the slepton case. This is as expected, because the neutralino annihilation is dominantly P -wave because of the Majorana-ness of neutralinos, while slepton annihilation takes place in the S -wave. In fact, for similar masses, one expects the slepton relic density to be suppressed relative to the neutralino relic density by a factor of roughly $v^2 \sim 3/x_F \sim 1/10$. Given the approximations used, this is in reasonable quantitative agreement with the estimates of Eqs. (33)–(36).

IV. CONSTRAINTS

A. Dark matter density

An unambiguous and simple constraint on these scenarios is that the resulting gravitino energy density should not be greater than the observed dark matter density. This constraint may be avoided if there is significant entropy production between NLSP freeze out and now. However, assuming such new physics is counter to our goal of evaluating the gravitino LSP possibility in the simplest possible cosmology, and so we require

$$\Omega_{\tilde{G}} h^2 = \frac{m_{\tilde{G}}}{m_{\text{NLSP}}} \Omega_{\text{NLSP}}^{\text{th}} h^2 < 0.11. \quad (37)$$

As evident from Eqs. (7) and (19) and Figs. 1 and 2, the typical decay times are $t \sim 10^4 - 10^8$ s. This is the natural decay time of a particle with weak-scale mass that decays through gravitational interactions. There are therefore additional constraints, most importantly from bounds on EM energy release from cosmic microwave background (CMB) μ distortions and from bounds on both EM and hadronic energy release from BBN light element abundances.

B. Cosmic microwave background

The CMB constraint is fairly straightforward to understand. The CMB photon energy distribution at times $t \lesssim 10^8$ s may be parameterized as

$$f_{\gamma}(E) = \frac{1}{e^{E/(kT)+\mu} - 1}, \quad (38)$$

with chemical potential μ . For early decays, EM cascades are completely thermalized through energy-changing processes $\gamma e^- \rightarrow \gamma e^-$ and number-changing interactions, such as $eX \rightarrow eX\gamma$, where X is an ion, and double Compton scattering $\gamma e^- \rightarrow \gamma\gamma e^-$. The resulting distribution is therefore Planckian, with $\mu = 0$. For decay times in the window of interest, however, the number-changing processes may be inefficient. In this case, the

spectrum cannot relax to a distribution determined by only one parameter, the temperature T . It therefore relaxes to statistical but not thermodynamic equilibrium, resulting in a Bose-Einstein distribution function with $\mu \neq 0$.

The value of the chemical potential μ may be approximated for small energy releases by analytic expressions given in Ref. [47]. These have been updated with current cosmological parameters in Ref. [18]. We will apply the current constraint [48,49]

$$|\mu| < 9 \times 10^{-5}. \quad (39)$$

C. Big bang nucleosynthesis

The BBN constraints are more complicated and more ambiguous. Constraints on EM energy release have been studied in [7,9,50–53]. Most recently, EM constraints (but not hadronic constraints) have been considered in Ref. [54] and these were used in the previous analyses of Refs. [17,18]. Here we include contours corresponding to the most stringent constraint from that analysis, the deuterium bound

$$1.3 \times 10^{-5} < D/H < 5.3 \times 10^{-5}, \quad (40)$$

to facilitate comparison with previous results.

More recently, both EM and hadronic energy releases have been bounded in the analysis of Ref. [23]. Of the constraints imposed there, the most relevant for us are the two σ bounds

$$2.4 \times 10^{-5} < D/H < 3.2 \times 10^{-5}, \quad (41)$$

$${}^3\text{He}/D < 1.13, \quad (42)$$

$${}^6\text{Li}/H < 6.1 \times 10^{-11}, \quad (43)$$

$$0.228 < Y_p < 0.248. \quad (44)$$

The statistical and systematic errors have been combined in quadrature for the ${}^4\text{He}$ (Y_p) constraint, and the ${}^6\text{Li}/H$ result is obtained by combining the 95% confidence level (CL) constraints ${}^6\text{Li}/{}^7\text{Li} = 0.05 \pm 0.02$ and ${}^7\text{Li}/H = 2.2_{-1.6}^{+6.5} \times 10^{-10}$ [55].

As is evident, the later analysis is much less conservative. First, it assumes a significantly more stringent D bound. Measurements of primordial D have long been considered by many to be the most reliable baryometers. There is also now impressive concordance between the baryon number determinations from D and CMB measurements, which further supports the narrow range of D/H given in Eq. (41). At the same time, existing discrepancies between standard BBN predictions and observations in other elements may indicate that caution is still needed in interpreting the D bound. In particular, if these discrepancies are indications of new physics, the required

new physics is also likely to distort the D abundance, since the D binding energy is so small.

The analysis of Ref. [23] also includes stringent constraints from ${}^3\text{He}/D$ and ${}^6\text{Li}/H$. If taken at face value, these additional bounds in fact provide some of the most stringent bounds on the gravitino LSP scenario. The ${}^3\text{He}/D$ bound is the strongest constraint on EM energy and provides the strongest constraint for NLSP decay times $\tau \gtrsim 10^7$ s, while the ${}^6\text{Li}/H$ constraint on hadronic energy release provides the strongest constraint on earlier decay times. At the same time, it is important to bear in mind that these constraints are on less sure footing than the D constraints. For ${}^3\text{He}$, ${}^3\text{He}/H$ suffers from uncertainties in chemical/stellar evolution [56]. Although ${}^3\text{He}/D$ has been proposed as an alternative tool to constrain new physics [51,57], present evaluations exist only in the Sun [58], and the determination of primordial ${}^3\text{He}/D$ requires a rather involved extrapolation of these results. ${}^6\text{Li}$ has also been proposed as a promising probe of new physics. However, after WMAP, there is a clear discrepancy between standard BBN predictions and the observations of ${}^7\text{Li}$ [59–61], with consistency possible only if systematic uncertainties have been underestimated [62]. This calls the status of ${}^6\text{Li}$ into question, as direct observations of ${}^6\text{Li}/H$ are difficult, and so the upper limit on ${}^6\text{Li}/H$ is usually derived from bounds on ${}^6\text{Li}/{}^7\text{Li}$. In fact, the current status of ${}^6\text{Li}$ and ${}^7\text{Li}$ may also be taken as evidence for new particle physics [63,64].

In light of all of these comments, we present constraint contours from all of these data, including both D constraints, to show the (strong) effect of varying BBN assumptions. We consider regions of parameter space that violate the conservative constraint of Eq. (40) to be excluded, but we consider regions that violate only Eqs. (41)–(43) to be at most disfavored, but not necessarily excluded, given the significant ambiguities noted above.

There are subtleties in importing the constraints of Eqs. (41)–(43) to the present analysis. When including both EM and hadronic energy release, there is the possibility of cancellations. In addition, although the EM constraint depends essentially only on ξ_{EM} of Eq. (5), the hadronic constraint may depend, in principle, ϵ_{had} and $B_{\text{had}} Y_{\text{NLSP}}$ separately, and results are presented only for a few values of ϵ_{had} . In practice, however, the cancellations occur only in rather special cases for particular energy release time. In addition, in supergravity with a gravitino LSP, the NLSP lifetime is usually larger than 150 sec, and so the hadronic constraint depends to a good approximation on $\xi_{\text{had}} \equiv \epsilon_{\text{had}} B_{\text{had}} Y_{\text{NLSP}}$ only.⁵ We therefore impose constraints on ξ_{had} and impose the constraints on EM and hadronic energy release separately, ignoring the possibility of cancellations.

⁵The constraint on ξ_{had} varies only by a factor of 2 for ϵ_{had} between 100 GeV and 1 TeV [55].

V. RESULTS

We have now determined the energy release parameters B_i and ϵ_i in Sec. II and Y_{NLSP} in Sec. III. We may now compare these to the constraints of Sec. IV to determine what combinations of gravitino mass and NLSP mass are excluded, disfavored, and allowed for various NLSP possibilities. We will present results in the $(m_{\tilde{G}}, \delta m)$ plane, where $\delta m \equiv m_{\text{NLSP}} - m_{\tilde{G}} - m_Z$. We consider only $\delta m > 0$, so three-body decays are therefore always kinematically possible. Of course, they are highly suppressed for small δm .

A. Slepton NLSP

We begin with the stau NLSP scenario. We assume the stau is right-handed. Neutralino and chargino parameters enter in the three-body decay widths. We take $\mu = M_2 = 2M_1 = 4m_{\tilde{\tau}_R}$ and $\tan\beta = 10$.

The results are presented in Fig. 3. To understand these results, it may be helpful to refer to the mass and lifetime contours of Fig. 1. Note that, given the definition of δm , $m_{\tilde{\tau}_R} > m_Z$ in the entire plane. The current limit on a metastable stau from LEP is $m_{\tilde{\tau}_R} > 99$ GeV [65], and so excludes a small portion of the lower lefthand corner.

The shaded regions are excluded. Given the scaling $\Omega_{\text{NLSP}}^{\text{th}} \propto m_{\text{NLSP}}^2$ for the thermal relic density, the dark matter density implies an upper bound on the product $m_{\text{NLSP}}m_{\tilde{G}}$, excluding $\tilde{\tau}$ and gravitino masses ~ 1 TeV. The constraint is relatively mild, because staus annihilate efficiently through S -wave processes. The other shaded region is excluded by the absence of CMB μ distortions. This provides a more stringent constraint than $\Omega_{\tilde{G}}$ for decay times $\tau \gtrsim 10^7$ s, when the decay products are produced too late to be thermalized.

The BBN sensitivity contours divided into those from D and ${}^4\text{He}$, which are probably the most reliable (left panel), and those from ${}^3\text{He}$ and ${}^6\text{Li}$, which are on less sure footing, given the discussion of Sec. IV C. For the D and ${}^4\text{He}$ results, we present results given the conservative bound of Eq. (40) on EM cascades (EM1), the more aggressive bound of Eqs. (41) and (44) on EM energy (EM2), and the bound of Eqs. (41) and (44) on hadronic cascades (had). The EM1 contour lies completely in the CMB-excluded region. Although BBN constraints are often assumed to be the leading constraint on late decays, we see that the CMB spectrum is now known to be Planckian to such high precision that the CMB constraint is competitive with the leading BBN constraints. At the same time, we see that the strength of the EM constraints in constraining gravitino LSP parameter space depends sensitively on how one interprets the BBN data. Adopting the more stringent EM2 contour, we find that bounds on $m_{\tilde{G}}$ are improved by about an order of magnitude.

Our analysis includes hadronic bounds on the gravitino LSP scenario for the first time. From Fig. 3, we see that

the hadronic constraint is the leading constraint for relatively early decays. Recall that sleptons produce hadronic energy only in three-body decays, and so the hadronic energy release is suppressed by factors of $\sim 10^{-3}$ relative to EM energy. Nevertheless, hadronic decay products are so lethal to light elements that the hadronic constraints are the most stringent constraint in parts of parameter space. Note also that the part of parameter space in which hadronic constraints are most important is where $m_{\tilde{\tau}_R}$ and $m_{\tilde{G}}$ are both in the hundreds of GeV, the most natural region for weak-scale supergravity. We conclude that hadronic constraints and three-body decays must be taken into account to establish the viability of any gravitino LSP scenario.

In the right panel of Fig. 3, we include the sensitivity contours of ${}^3\text{He}$ and ${}^6\text{Li}$. We see that, taken literally, the constraint on ${}^3\text{He}$ provides the most stringent constraint on late decays (through its limits on EM energy) and ${}^6\text{Li}$ provides the leading constraint on early decays (through its limits on hadronic energy). Of course, given the ambiguities discussed in Sec. IV C, we do not consider these contours to be exclusion contours. These sensitivity contours are of interest, however, as, if colliders measure the superpartner parameters to be in the regions to the right of these contours (as we will discuss in Sec. VI), these measurements will have important implications for BBN.

Last, we discuss the dark matter implications of these results. At the boundary of the region excluded by $\Omega_{\tilde{G}}$, the light (yellow) shaded region, gravitino superWIMPs account for all of dark matter. Taking the EM1 and hadronic constraints from D and ${}^4\text{He}$, we see that this possibility is indeed viable. If, however, the various BBN anomalies are resolved and the EM2 and ${}^3\text{He}$ and ${}^6\text{Li}$ contours may be considered as exclusion contours, the possibility that superWIMP gravitinos form all of dark matter may be excluded. However, given the current status of BBN, we find such conclusions premature.

Finally, we should remind the reader that we have assumed a particular thermal relic density and particular neutralino mass parameters, which enter the three-body branching ratios. All of the contours above will shift if there are significant deviations in these assumptions. A complete analysis of all of these variations is, however, beyond the scope of this work.

B. Sneutrino NLSP

As discussed in Sec. II B, if the NLSP is a sneutrino, two-body decays are essentially invisible, and so inclusion of three-body decays is essential to determine the viable parameter space. Because the hadronic constraints are some much stronger than the EM constraints, we may focus on them only. Again, neutralino and chargino parameters enter in the three-body decay widths, and we assume $\mu = M_2 = 2M_1 = 4m_{\tilde{\nu}}$ and $\tan\beta = 10$.

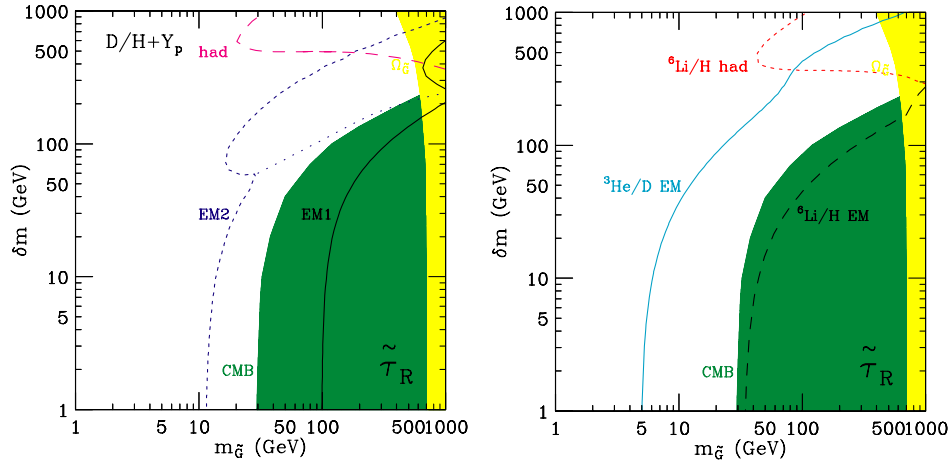


FIG. 3 (color online). Excluded and allowed regions of the $(m_{\tilde{G}}, \delta m \equiv m_{\text{NLSP}} - m_{\tilde{G}} - m_Z)$ parameter space in the gravitino LSP scenario, assuming a $\tilde{\tau}_R$ NLSP that freezes out with thermal relic density given by Eq. (33). The light (yellow) shaded region is excluded by the overclosure constraint $\Omega_{\tilde{G}} h^2 < 0.11$, and the medium (green) shaded region is excluded by the absence of CMB μ distortions. BBN is sensitive to the regions to the right of the labeled contours. Left: Regions probed by D and ${}^4\text{He}$, assuming the conservative result of Eq. (40) (EM1), and the more stringent constraints of Eqs. (41) and (44) (EM2 and had). The dotted line denotes the region where cancellation between D destruction and creation via late time EM injection is possible [27], while ${}^7\text{Li}$ is reduced to the observed value by the late NLSP decays [54]. Right: Regions probed by ${}^3\text{He}/\text{D}$ (EM), ${}^6\text{Li}/\text{H}$ (had) [23], and ${}^6\text{Li}/\text{H}$ (EM) [23,54].

The results are presented in Fig. 4. Sneutrinos annihilate through S -wave processes even more efficiently than sleptons, as can be seen by comparing Eqs. (33) and (34). The dark matter density bound is therefore weaker, and is in fact pushed to the right; it does not appear in the plotted plane. The CMB constraint, previously so strin-

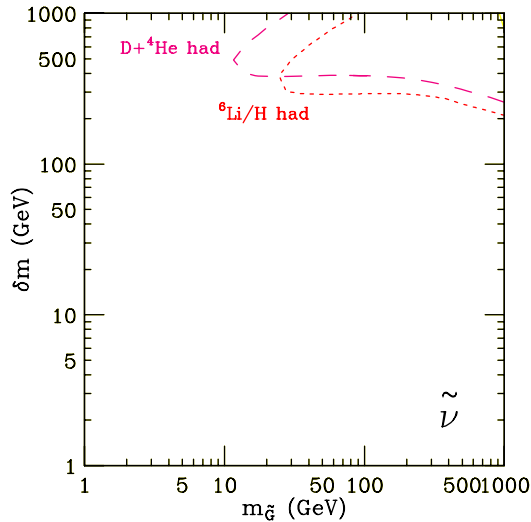


FIG. 4 (color online). As in Fig. 3, but assuming a sneutrino NLSP that freezes out with thermal relic density given by Eq. (34).

gent, is also absent, of course, as it constrains EM energy, and the BBN constraints on EM energy are also absent.

The remaining constraints are therefore only the hadronic BBN constraints. These are stringent for early decays, that is, large δm . The more reliable D and ${}^4\text{He}$ constraints disfavor $\delta m \gtrsim 300$ GeV, while ${}^6\text{Li}$ (had) is sensitive to $\delta m \gtrsim 200$ GeV. It is rather remarkable that the sneutrino NLSP case is so tightly constrained, given its invisible dominant decay mode. At the same time, the scenario is perfectly viable for natural weak-scale supergravity parameters. Note that gravitino superWIMP dark matter is also viable for $m_{\tilde{G}} \sim 1$ TeV and $\delta m \lesssim 300$ GeV.

C. Bino NLSP

Finally, we turn to the case of the Bino NLSP. The results are presented in Fig. 5 for the case where the Bino thermal relic density is as in the bulk region of minimal supergravity [Eq. (35)], and in Fig. 6 for the case where the Bino relic density is degraded by a factor of 4 [Eq. (36)], as might be the case if there are additional effects as may be found in the focus point or coannihilation regions of minimal supergravity. Note that the $m_{\tilde{G}}$ lower limit has been extended to much lower masses than in the slepton and sneutrino figures. The mass and lifetime contours of Fig. 2 may be helpful in understanding these results.

The CMB and EM BBN bounds are roughly similar to those in the slepton NLSP case. However, for the other bounds, there are important changes. Because neutralino

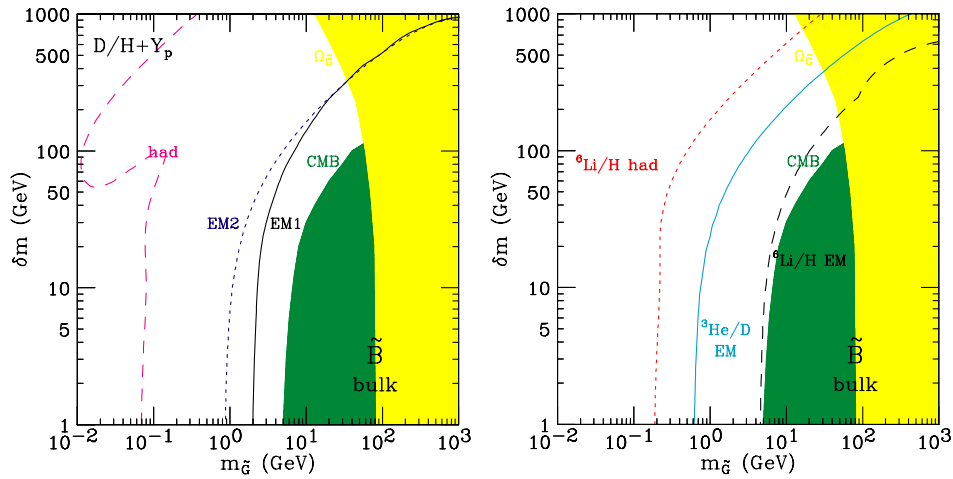


FIG. 5 (color online). As in Fig. 3, but assuming a Bino NLSP that freezes out with the bulk thermal relic density given by Eq. (35).

annihilation is P -wave suppressed, the dark matter density limit is much more stringent, excluding gravitino masses above 100 GeV and 200 GeV in the bulk and “FP/coann” cases, respectively.

Even more striking, the hadronic BBN bounds become much more stringent. This is expected—Bino NLSP decays contribute to hadronic energy at the two-body level through decays $\tilde{B} \rightarrow Z\tilde{G}$. The branching fractions for EM and hadronic decays are therefore not too different, and the extreme stringency of the hadronic constraints makes them the dominant bound. Taking only the relatively reliable D and ${}^4\text{He}$ bounds, we find that decay times $\tau \geq 10^3$ s are disfavored, excluding almost all gravitino masses $m_{\tilde{G}} \geq 100$ MeV. In the FP/coann case, for $\delta m \lesssim \mathcal{O}(10$ GeV), the hadronic constraints exclude $100 \lesssim m_{\tilde{G}} \lesssim 500$ MeV, but $m_{\tilde{G}} \sim 1$ GeV is again allowed. In

the allowed region, the decay times are so long $\tau \approx 10^5$ s that the hadronic constraints become less stringent. However, for such long decays, the EM constraints are stringent. As can be seen in the figures, the EM constraints disfavor or exclude this island of parameter space, depending on how conservative one’s interpretation of the EM BBN constraints is.

We therefore conclude that hadronic BBN constraints essentially exclude supergravity with a gravitino LSP and a Bino NLSP when the decay channel $\tilde{B} \rightarrow Z\tilde{G}$ is open. The Bino NLSP scenario is viable only if the Bino and gravitino masses are degenerate enough to suppress this decay mode, if $m_{\tilde{G}}$ is below 10 MeV, a rather unnatural value of conventional supergravity, or, possibly, if there are extremely coannihilation effects which suppress the thermal relic density even more than in our FP/coann

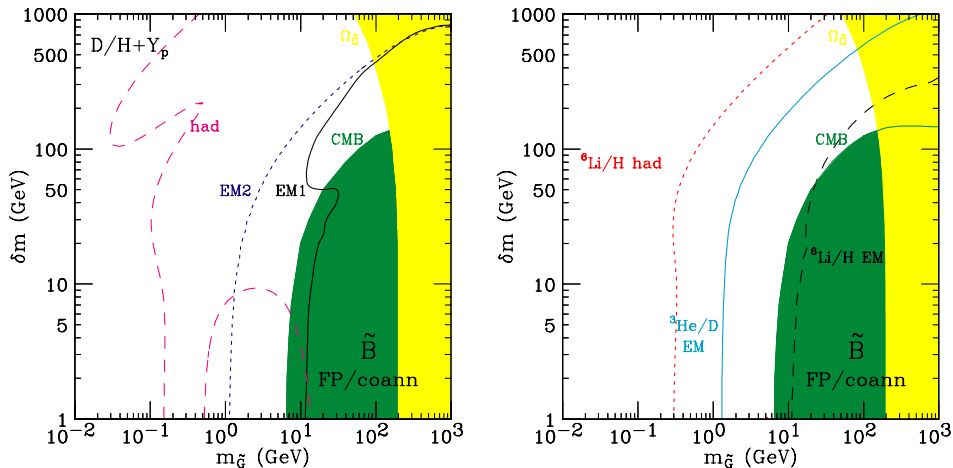


FIG. 6 (color online). As in Fig. 3, but assuming a Bino NLSP that freezes out with the “focus point/coannihilation” thermal relic density given by Eq. (36). In the left panel, the region between the “had” lines is disfavored.

example. If the neutralino NLSP is not pure Bino, there are additional possibilities. For example, as noted in Ref. [18], photino NLSPs may be viable, as they contribute to hadronic cascades only through three-body decays. Of course, from the high-energy viewpoint, a photinlike neutralino is unmotivated. More likely is the case of a Higgsino-gaugino neutralino, for which the thermal relic density may also be greatly suppressed, but the hadronic constraints are stronger, since $\Gamma(\chi \rightarrow h\tilde{G})$ is larger. A detailed examination of such focus point or coannihilation cases would be interesting, but is beyond the scope of this study.

VI. IMPLICATIONS FOR COLLIDER PHYSICS

The possibility of a gravitino LSP in supergravity has rich implications for current and future colliders. These implications depend crucially on whether the NLSP is a slepton, sneutrino, or neutralino. In all cases, however, given NLSP rest lifetimes of $10^4 - 10^8$ s, the typical NLSP decay lengths are enormous relative to collider detectors, and so these NLSPs are essentially stable as far as colliders are concerned.

A. Slepton NLSP

We begin by discussing the slepton NLSP case. This possibility is very natural from the point of view of high-energy frameworks. Given simple boundary conditions at the grand unified scale, for example, and evolving these to the weak-scale, right-handed sleptons, in particular, right-handed staus, often emerge as the lightest standard model superpartner. In conventional studies of these high-energy frameworks, such regions of parameter space are excluded by bounds from searches for charged massive stable particles in sea water. In the gravitino LSP scenario, however, the lightest slepton is metastable but not absolutely stable, and so these bounds do not apply.

The excluded and allowed regions of parameter space are presented again in Fig. 7, but now in the $(m_{\tilde{G}}, m_{\tilde{\tau}_R})$ plane, which is more convenient for inferring implications for colliders. We see that, allowing the gravitino to be as light as 10 GeV, all weak-scale stau masses are allowed. Staus may therefore be within reach of the LHC and even of the first stage of a linear collider. For heavier gravitino masses, the allowed stau mass range becomes more narrow. Neglecting the aggressive EM2 bound, we see that all dark matter may be in the form of gravitino superWIMPs if staus have masses $m_{\tilde{\tau}_R} \gtrsim 1$ TeV. In this case, direct stau production is beyond the range of the LHC and linear collider, but staus may still be produced in the cascade decays of squarks and gluinos.

At hadron colliders, sleptons can be pair-produced through the Drell-Yan processes

$$q\bar{q}' \rightarrow W^* \rightarrow \tilde{l}_L \bar{\nu}_L, \quad (45)$$

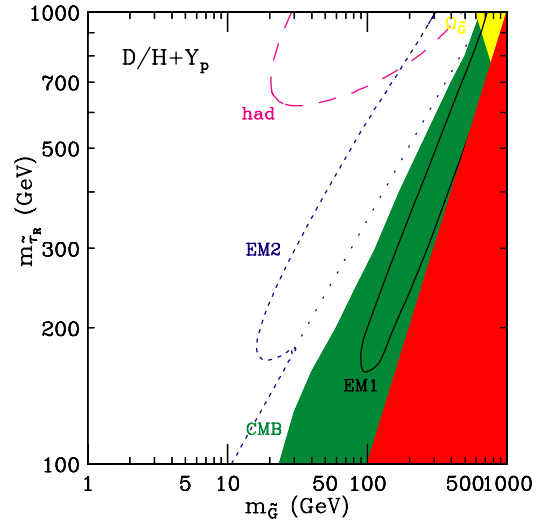


FIG. 7 (color online). Excluded and allowed regions for the gravitino LSP scenario, assuming a $\tilde{\tau}_R$ NLSP, as in the left panel of Fig. 3, but now in the $(m_{\tilde{G}}, m_{\tilde{\tau}_R})$ plane. In the dark (red) shaded region the gravitino is not the LSP. All other shaded regions and contours are as in Fig. 3.

$$q\bar{q} \rightarrow Z^*, \gamma^* \rightarrow \tilde{l}_L \bar{\nu}_L, \tilde{l}_R \bar{l}_R, \tilde{\nu}_L \bar{\nu}_L. \quad (46)$$

The cross sections for such processes are determined by the slepton masses, with very little other model dependence.⁶ These Drell-Yan cross sections have been studied in detail [66–68], including the leading QCD corrections. For the Tevatron with $\sqrt{s} = 2$ TeV and $m_{\tilde{l}} = 100$ GeV, the cross sections for $\tilde{l}_R \bar{l}_R$, $\tilde{l}_L \bar{l}_L$ ($\tilde{\nu}_L \bar{\nu}_L$), and $\tilde{l}_L \bar{\nu}_L$ are about 10 fb, 30 fb, and 100 fb, respectively. These cross sections drop quickly for heavier sleptons. For $m_{\tilde{l}} = 200$ GeV, they are reduced by more than an order of magnitude, and sleptons with mass above around 250 GeV will be beyond the reach of the Tevatron.

For the LHC with $\sqrt{s} = 14$ TeV, the Drell-Yan cross sections are about 10 times bigger. Sleptons may also be produced via weak boson fusion [69],

$$qq' \rightarrow qq'VV \rightarrow qq'\tilde{l}\tilde{l}. \quad (47)$$

This cross section decreases much more slowly with increasing slepton mass than the Drell-Yan cross section, and the weak boson fusion cross section dominates for $m_{\tilde{l}} \gtrsim 200 - 300$ GeV. At the LHC, hundreds to thousands of sleptons could be produced.

Metastable sleptons will appear as charged tracks in the tracking chamber with little calorimeter activity. Eventually they will hit the muon chambers and so look muonlike. However, given their large mass, such sleptons

⁶Much larger cross sections may result from sleptons produced in cascade decays of gluinos and squarks, but the details of these processes are highly model-dependent.

may be nonrelativistic. They can therefore be highly ionizing, allowing one to distinguish them from genuine muons. In addition, time-of-flight information could be used to detect a slow moving particle. Such signals are almost background free, providing the potential for a spectacular signature [70–72].

Searches for metastable sleptons have been motivated previously by the existence of such particles in gauge-mediated supersymmetry breaking models [66,72–75]. No signals have been found at Tevatron Runs I and II [76] and LEP [65]. The most stringent current bound is $m_{\tilde{l}} > 99$ GeV at 95% CL from LEP searches at center-of-mass energies up to 208 GeV. The prospects for a full Tevatron Run II have been investigated in Ref. [66], where appropriate cuts in slepton velocity and pseudorapidity η have been included to eliminate the background. Requiring five or more events for a signal, the estimated reach in right-handed slepton mass is about 110 GeV, 180 GeV, and 230 GeV for integrated luminosities of 2, 10, and 30 fb^{-1} , respectively. The discovery reach of the LHC has also been considered [77]. For 1 yr at the design luminosity of 100 fb^{-1} , metastable sleptons with mass up to 700 GeV could be discovered.

As noted above, metastable sleptons are possible in both the high-scale supersymmetry breaking scenarios discussed here, and in low-scale supersymmetry breaking models, such as those with gauge-mediated supersymmetry breaking. In the gauge-mediated scenarios, however, the gravitino mass is much lighter, around the keV scale. It is possible that these cases may be distinguished cosmologically. Alternatively, direct collider searches for other supersymmetric particles and the measurement of their mass spectra will provide additional means for distinguishing these possibilities. Finally, the slepton lifetimes in gauge-mediated models, although long on collider detector scales, are much shorter than in the superWIMP scenarios discussed here, and this may be distinguished experimentally, providing an unambiguous determination [78].

B. Sneutrino and neutralino NLSP

The cases of a gravitino LSP with either a sneutrino or neutralino NLSP are qualitatively different from the slepton NLSP case. The allowed regions of parameter space are given in Figs. 8 and 9. In both cases, the metastable NLSP will pass through detectors, resulting in missing energy signatures topologically identical to the conventional missing energy signal of supersymmetry. There are four cases to distinguish: the lightest standard model superpartner may be either a sneutrino or a neutralino, and this particle may either decay to a gravitino or not.

The sneutrino and neutralino cases may be distinguished by precision supersymmetry studies at colliders. For example, in e^+e^- collisions, the signatures of slepton

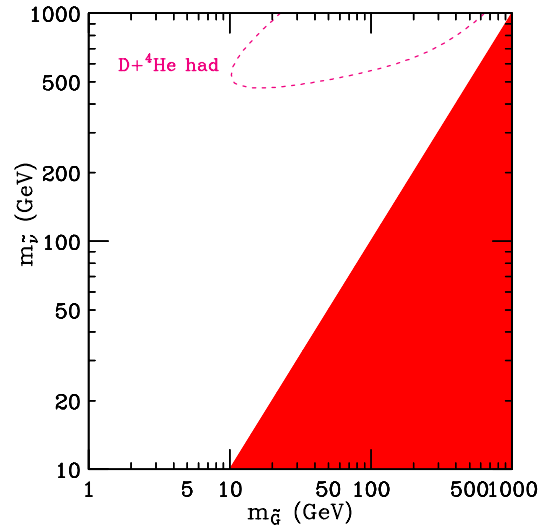


FIG. 8 (color online). Excluded and allowed regions for the gravitino LSP scenario, assuming a $\tilde{\nu}$ NLSP, as in Fig. 4, but now in the $(m_{\tilde{g}}, m_{\tilde{\nu}})$ plane. In the dark (red) shaded region the gravitino is not the LSP. The $D + {}^4\text{He}$ contour is as in Fig. 4.

pair production in the sneutrino scenario (for example, $e^+e^- \rightarrow \tilde{l}\tilde{l} \rightarrow l\nu\tilde{\nu}q\tilde{q}'\tilde{\nu}$) are identical to the signatures of chargino production in the neutralino scenario (for example, $e^+e^- \rightarrow \tilde{\chi}^+\tilde{\chi}^- \rightarrow l\nu\tilde{\chi}^0q\tilde{q}'\tilde{\chi}^0$) [79]. However, these possibilities may be distinguished easily through angular distributions at a linear collider, and possibly also at the LHC.

Determining whether the sneutrino or neutralino eventually decays to a gravitino may be more difficult. In the sneutrino case, the working assumption would be that the gravitino is the LSP—the sneutrino itself is disfavored as a dark matter candidate, because, in the natural region of parameter space, it predicts dark matter signals that have not been seen. On the other hand, in the neutralino case, the working assumption would be that the neutralino is stable—as we have seen, decays to the gravitino are highly constrained by hadronic BBN bounds. Further information will be provided by high sensitivity collider and astrophysical experiments. For example, a positive detection in dark matter search experiments would eliminate the possibility of a gravitino LSP. On the other hand, the precise determination of supersymmetry parameters will make possible the determination of the thermal relic abundance of the lightest standard model superpartner. This will favor the gravitino LSP scenario if this thermal relic density is larger than the observed dark matter density.

The current experimental limit on the sneutrino mass, assuming three degenerate families, is $m_{\tilde{\nu}} > 44.6$ GeV at 95% CL from limits on the invisible decay width of the Z [80]. The metastable sneutrino scenario has not been well studied. The collider signals and detector reaches depend

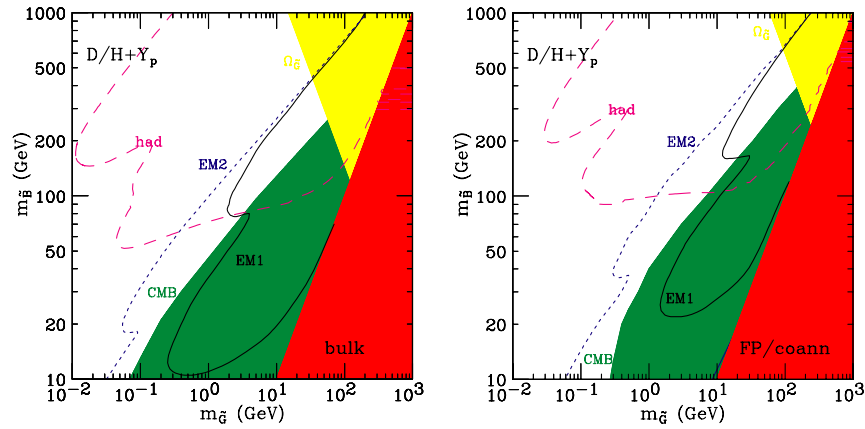


FIG. 9 (color online). Excluded and allowed regions for the gravitino LSP scenario, assuming a \tilde{B} NLSP in the $(m_{\tilde{G}}, m_{\tilde{B}})$ plane. In the (dark) red shaded region the gravitino is not the LSP. All other shaded regions and contours are as in the left panel of Fig. 5 (left) and as in the left panel of Fig. 6 (right).

crucially on the identity of the second lightest sparticle (which decays into the sneutrino), the accompanying decay products, experimental cuts and details of the detector. A detailed study of the collider phenomenology of the sneutrino scenario will appear in a future work.

VII. SUMMARY AND OUTLOOK

In this paper, we have determined the viability of supergravity scenarios in which the gravitino is the LSP. We have considered the three possibilities in which the NLSP is a slepton, a sneutrino, and a neutralino. In each case, we determined the branching fractions of the leading two- and three-body decays, and applied constraints from the dark matter density, CMB, and both EM and hadronic BBN bounds. We found that the hadronic BBN constraints, previously neglected, are extremely important, providing the most stringent limits in natural regions of parameter space.

The gravitino LSP scenario opens up many connections between particle physics and cosmology. Consider, for example, the slepton NLSP scenario. At colliders, it may be possible to collect the less energetic metastable sleptons in a detector and monitor this detector for slepton decays. By measuring the decay time distribution and the energy of each produced lepton, one could independently determine both the gravitino mass and the reduced Planck mass M_* [29,30].

A measurement of the gravitino mass determines the scale of supersymmetry breaking, with implications for model building and dark energy. At the same time, such a measurement would determine a particular place in the

$(m_{\tilde{G}}, m_{\text{NLSP}})$ plane. Colliders would therefore shed light on the possible role of such new physics in BBN, and more generally in the thermal history of the Universe after NLSP freeze out at temperatures of around 10 GeV. For example, the μ parameter sensitivity of Eq. (39) may be improved by 2 orders of magnitude in the future by the DIMES mission [81]. Such improvement would extend the CMB sensitivity contour significantly. The measurement of a μ distortion consistent with the determination of $(m_{\tilde{G}}, m_{\text{NLSP}})$ would provide a striking confirmation of the underlying gravitino scenario.

The measurement of M_* would provide a precision test of the supersymmetry predictions relating the properties of gravitinos to those of gravitons, and also provide the first direct measurement of the Planck scale on microscopic scales [29,30]. The crucial question is the feasibility of collecting a sizable sample of metastable NLSPs. There has been an earlier study on the collection of very long lived heavy charged leptons [71]. A more detailed analysis of the trapping of sleptons at future colliders is also now under study [78].

ACKNOWLEDGMENTS

We thank K. Kohri, T. Moroi, Y. Santoso, and V. Spanos for helpful correspondence. F.T. thanks Y. Santoso for useful discussions about the stau thermal relic abundance in supergravity models. The work of J. L. F. was supported in part by National Science Foundation CAREER Grant No. PHY-0239817, and in part by the Alfred P. Sloan Foundation.

- [1] H. Pagels and J.R. Primack, *Phys. Rev. Lett.* **48**, 223 (1982).
- [2] S. Weinberg, *Phys. Rev. Lett.* **48**, 1303 (1982).
- [3] L. M. Krauss, *Nucl. Phys.* **B227**, 556 (1983).
- [4] D.V. Nanopoulos, K. A. Olive, and M. Srednicki, *Phys. Lett. B* **127**, 30 (1983).
- [5] M.Y. Khlopov and A. D. Linde, *Phys. Lett. B* **138**, 265 (1984).
- [6] J. R. Ellis, J. E. Kim, and D.V. Nanopoulos, *Phys. Lett. B* **145**, 181 (1984).
- [7] J. R. Ellis, D.V. Nanopoulos, and S. Sarkar, *Nucl. Phys.* **B259**, 175 (1985).
- [8] R. Juszkiewicz, J. Silk, and A. Stebbins, *Phys. Lett. B* **158**, 463 (1985).
- [9] J. R. Ellis, G. B. Gelmini, J. L. Lopez, D.V. Nanopoulos, and S. Sarkar, *Nucl. Phys.* **B373**, 399 (1992).
- [10] T. Moroi, H. Murayama, and M. Yamaguchi, *Phys. Lett. B* **303**, 289 (1993).
- [11] M. Bolz, A. Brandenburg, and W. Buchmuller, *Nucl. Phys.* **B606**, 518 (2001).
- [12] For a review of cosmological constraints on late decays, see M.Y. Khlopov, *Cosmoparticle Physics* (World Scientific, Singapore, 1999).
- [13] L. Covi, J.E. Kim, and L. Roszkowski, *Phys. Rev. Lett.* **82**, 4180 (1999).
- [14] L. Covi, H. B. Kim, J.E. Kim, and L. Roszkowski, *J. High Energy Phys.* 0105 (2001), 033.
- [15] X. J. Bi, M.-Z. Li, and X.-M. Zhang, *Phys. Rev. D* **69**, 123521 (2004).
- [16] D. Hooper and L. T. Wang, hep-ph/0402220.
- [17] J. L. Feng, A. Rajaraman, and F. Takayama, *Phys. Rev. Lett.* **91**, 011302 (2003).
- [18] J. L. Feng, A. Rajaraman, and F. Takayama, *Phys. Rev. D* **68**, 063504 (2003).
- [19] J. L. Feng, S. Su, and F. Takayama, *Phys. Rev. D* **70**, 063514 (2004).
- [20] J. L. Feng, A. Rajaraman, and F. Takayama, *Phys. Rev. D* **68**, 085018 (2003).
- [21] X. Chen and M. Kamionkowski, *Phys. Rev. D* **70**, 043502 (2004).
- [22] K. Sigurdson and M. Kamionkowski, *Phys. Rev. Lett.* **92**, 171302 (2004).
- [23] M. Kawasaki, K. Kohri, and T. Moroi, astro-ph/0402490.
- [24] M. Fujii, M. Ibe, and T. Yanagida, *Phys. Lett. B* **579**, 6 (2004).
- [25] M. H. Reno and D. Seckel, *Phys. Rev. D* **37**, 3441 (1988).
- [26] S. Dimopoulos, R. Esmailzadeh, L. J. Hall, and G. D. Starkman, *Astrophys. J.* **330**, 545 (1988).
- [27] S. Dimopoulos, R. Esmailzadeh, L. J. Hall, and G. D. Starkman, *Nucl. Phys.* **B311**, 699 (1989).
- [28] K. Kohri, *Phys. Rev. D* **64**, 043515 (2001).
- [29] W. Buchmuller, K. Hamaguchi, M. Ratz, and T. Yanagida, *Phys. Lett. B* **588**, 90 (2004).
- [30] J. L. Feng, A. Rajaraman, and F. Takayama, hep-th/0405248.
- [31] J. R. Ellis, K. A. Olive, Y. Santoso, and V. Spanos, *Phys. Lett. B* **588**, 7 (2004).
- [32] T. Moroi, hep-ph/9503210.
- [33] J. Bernstein, L. S. Brown, and G. Feinberg, *Phys. Rev. D* **32**, 3261 (1985).
- [34] R. J. Scherrer and M. S. Turner, *Phys. Rev. D* **33**, 1585 (1986); **34**, 3263E (1986).
- [35] T. Asaka, K. Hamaguchi, and K. Suzuki, *Phys. Lett. B* **490**, 136 (2000).
- [36] J. L. Feng and T. Moroi, *Phys. Rev. D* **61**, 095004 (2000).
- [37] J. L. Feng, K. T. Matchev, and T. Moroi, *Phys. Rev. Lett.* **84**, 2322 (2000).
- [38] J. L. Feng, K. T. Matchev, and T. Moroi, *Phys. Rev. D* **61**, 075005 (2000).
- [39] S. Mizuta and M. Yamaguchi, *Phys. Lett. B* **298**, 120 (1993).
- [40] J. L. Feng, K. T. Matchev, and F. Wilczek, *Phys. Lett. B* **482**, 388 (2000).
- [41] J. L. Feng, K. T. Matchev, and F. Wilczek, *Phys. Rev. D* **63**, 045024 (2001).
- [42] P. Binetruy, G. Girardi, and P. Salati, *Nucl. Phys.* **B237**, 285 (1984).
- [43] K. Griest and D. Seckel, *Phys. Rev. D* **43**, 3191 (1991).
- [44] J.R. Ellis, T. Falk, K. A. Olive, and M. Srednicki, *Astropart. Phys.* **13**, 181 (2000); **15**, 413E (2001).
- [45] R. Arnowitt, B. Dutta, and Y. Santoso, *Nucl. Phys.* **B606**, 59 (2001).
- [46] T. Nihei, L. Roszkowski, and R. Ruiz de Austri, *J. High Energy Phys.* 0207 (2002), 024.
- [47] W. Hu and J. Silk, *Phys. Rev. Lett.* **70**, 2661 (1993).
- [48] D.J. Fixsen *et al.*, *Astrophys. J.* **473**, 576 (1996).
- [49] Particle Data Group Collaboration, K. Hagiwara *et al.*, *Phys. Rev. D* **66**, 010001 (2002).
- [50] M. Kawasaki and T. Moroi, *Astrophys. J.* **452**, 506 (1995).
- [51] E. Holtmann, M. Kawasaki, K. Kohri, and T. Moroi, *Phys. Rev. D* **60**, 023506 (1999).
- [52] M. Kawasaki, K. Kohri, and T. Moroi, *Phys. Rev. D* **63**, 103502 (2001).
- [53] T. Asaka, J. Hashiba, M. Kawasaki, and T. Yanagida, *Phys. Rev. D* **58**, 023507 (1998).
- [54] R. H. Cyburt, J. R. Ellis, B. D. Fields, and K. A. Olive, *Phys. Rev. D* **67**, 103521 (2003).
- [55] K. Kohri (private communication).
- [56] E. Vangioni-Flam, K. A. Olive, B. D. Fields, and M. Casse, *Astrophys. J.* **585**, 611 (2003).
- [57] G. Sigl, K. Jedamzik, D. N. Schramm, and V. S. Berezinsky, *Phys. Rev. D* **52**, 6682 (1995).
- [58] S. T. Scully, M. Casse, K. A. Olive, D. N. Schramm, J. Truran, and E. Vangioni-Flam, *Astrophys. J.* **462**, 960 (1996).
- [59] J. A. Thorburn, *Astrophys. J.* **421**, 318 (1994).
- [60] P. Bonifacio and P. Molaro, *Mon. Not. R. Astron. Soc.*, **285**, 847 (1997).
- [61] S. G. Ryan, T. C. Beers, K. A. Olive, B. D. Fields, and J. E. Norris, *Astrophys. J. Lett.* **530**, L57 (2000).
- [62] R. H. Cyburt, B. D. Fields, and K. A. Olive, *Phys. Rev. D* **69**, 123519 (2004).
- [63] K. Jedamzik, *Phys. Rev. Lett.* **84**, 3248 (2000).
- [64] K. Jedamzik, *Phys. Rev. D* **70**, 063524 (2004).
- [65] LEPUSYWG, ALEPH, DELPHI, L3, and OPAL experiments, Note LEPUSYWG/02-05.1 (<http://lepsusy-web.cern.ch/lepsusy/Welcome.html>).
- [66] J. L. Feng and T. Moroi, *Phys. Rev. D* **58**, 035001 (1998).
- [67] H. Baer, B. W. Harris, and M. H. Reno, *Phys. Rev. D* **57**, 5871 (1998).

- [68] W. Beenakker, M. Klasen, M. Kramer, T. Plehn, M. Spira, and P. M. Zerwas, *Phys. Rev. Lett.* **83**, 3780 (1999).
- [69] D. Choudhury, A. Datta, K. Huitu, P. Konar, S. Moretti, and B. Mukhopadhyaya, *Phys. Rev. D* **68**, 075007 (2003).
- [70] M. Drees and X. Tata, *Phys. Lett. B* **252**, 695 (1990).
- [71] J. L. Goity, W. J. Kossler, and M. Sher, *Phys. Rev. D* **48**, 5437 (1993).
- [72] A. Nisati, S. Petrarca, and G. Salvini, *Mod. Phys. Lett. A* **12**, 2213 (1997).
- [73] S. Ambrosanio, G. D. Kribs, and S. P. Martin, *Phys. Rev. D* **56**, 1761 (1997).
- [74] P. G. Mercadante, J. K. Mizukoshi, and H. Yamamoto, *Phys. Rev. D* **64**, 015005 (2001).
- [75] S. Ambrosanio, B. Mele, S. Petrarca, G. Polesello, and A. Rimoldi, *J. High Energy Phys.* 0101 (2001), 014.
- [76] CDF Collaboration and D0 Collaboration, K. Hoffman, hep-ex/9712032; CDF collaboration, C. Pagliarone, hep-ex/0312005.
- [77] D. Acosta, Proceedings of the 14th Topical Conference on Hadron Collider Physics, September 29–October 4, 2002, Germany (unpublished).
- [78] J. L. Feng, H. Murayama, and B. T. Smith (to be published).
- [79] A similar confusion with sneutrino LSP scenarios has been previously noted in A. de Gouvea, A. Friedland, and H. Murayama, *Phys. Rev. D* **59**, 095008 (1999).
- [80] T. Hebbeker, *Phys. Lett. B* **470**, 259 (1999).
- [81] <http://map.gsfc.nasa.gov/DIMES>.